**2018 14th IEEE International Conference on Control & Automation (ICCA)**
**June 12-15, 2018, Anchorage, Alaska, USA**

# Surface Pressure Reconstruction for a Prosthetic Socket Design System - a Numerical Case Study

W. Xu[1], A. van Heesewijk[1], M Tayler[1], X Zhu, L. Lorenzelli[2], V. Papadimitriou[3], A. S. Haidar[4] and J. Gao[5]

[1] University of Surrey, [2] Fondazione Bruno Kessler, [3] Innora, [4] London Prosthetic Centre, [5] TWI Limited

***Abstract* - A prosthetic socket connects the residual limb of amputee with a prosthesis. The comfort of a prosthesis user depends on the socket design because, through the socket, the body weight and its associated moment during walking, running or climbing are transmitted to the artificial limb. In the current clinical practices, a prosthetic socket is designed using a touch-and-feel approach by a well-trained prosthetist which is a highly subjective process. In order to achieve optimized design of a socket for individual amputees, an integrated sensors system is developed for above knee amputees. In this paper a numerical simulation based reverse engineering approach is used to obtain average surface pressure distribution on the residual limb from the measurements of a limited number of tri-axial force sensor array we developed.**

## I. INTRODUCTION

As an important part, a prosthetic socket connects the residual limb of an amputee with an artificial prosthesis. The prosthetic socket is regarded as the most critical component which determines the comfort of patients, the lower limb amputees in particular, when they wear the prosthesis in their daily lives. Through the socket, the amputee's body weight and the dynamic load are distributed and transmitted to the prosthesis during walking, running or climbing.

Based on 14 years' experience with 290 prostheses, Botta and Baumgartner reported that the production of a prosthetic socket is achieved by a touch-and-feel method which is conducted by a well-trained prosthetist [1]. In this case it primarily depends on the skill and experiences of the prosthetist, and is a highly subjective process.

Although there has been significant progress in the development of prosthetic technologies such as microprocessor supported knee and ankle joints in the recent years [2], the development of a comfortable socket has been left behind due to the complexity of the residual limb under loading (walking) conditions. As a result, the current way of producing a prosthetic socket is still very time-consuming, yet the quality of outcome is difficult to guarantee.

In recent years, efforts have been made in the development of the sensors to meet the requirement of pressure and shear force measurement inside the prosthetic socket [3 &4]. However, these developments only reported individual case of pressure and shear force measurement using different types of sensors which were yet to be integrated into the prosthetic socket and with limited coverage over the socket area of the residual limb.

With support of the state-of-the-art sensor and MEMS technologies, a new prosthetic socket design system has been developed. This system is expected to enable prosthetists to achieve rapid design and production of the comfortable socket for the above knee amputees [5 & 6]. However, the drawback of this newly developed sensor is that it can only provide local pressure and shear force measurement around the area of each individual sensor.

In this paper, we firstly present a tri-axial force sensor which is developed for pressure and shear stress measurement for prosthetic socket design [7 & 8]. It is followed by a brief presentation of the socket design system itself, before we discuss the reconstruction of average surface pressure distribution from an individual sensor measurement using a numerical simulation based reverse engineering approach. Finally, to establish the relationship between an individual sensor measurement and average surface pressure, regressions were carried out on the data obtained from the numerical simulations.

## II. SENSOR AND SOCKETMASTER SYSTEM

### *A. Development of Tri-axial Force Sensor*

In order to achieve both pressure and friction measurement, the priority has been given to the MEMS based sensor which consists of a force sensor array with five silicon thin membranes as sensitive areas. The force on each membrane due to an applied load can be measured by means of a Wheatstone bridge formed by four piezo-resistors.

The chip surface is embedded under a polymeric dome so that normal and shear forces applied on the surface of the sensor can be recorded. The sensor is set on a two-side printed circuit board (PCB) with a read out electronic circuit and a microcontroller for data processing through an $I^2C$ communication standard.

According to the system architecture designed, each sensing unit is an independent module consisting of five MEMS piezo-resistive force sensors, with temperature sensors, read out electronics, processing unit, transmission bus mounted on a PCB

This research is supported by the SocketMaster project which is funded by the European Union's Horizon 2020 for research and innovation program under grant agreement no. 645239.

Corresponding author: W. Xu, Centre for biomedical engineering, University of Surrey, Guildford, Surrey, UK GU2 7XH. Email:w.xu@surrey.ac.uk.

with dimensions of 2.78×4.3 $cm^2$. The five sensor chips have been connected to the read out electronics via standard ball bonding contacts. The schematic of Figure 1 shows the overall system architecture of the developed sensor. A customized polymeric dome is bonded on the top of the sensing unit to achieve normal and shear force measurement.

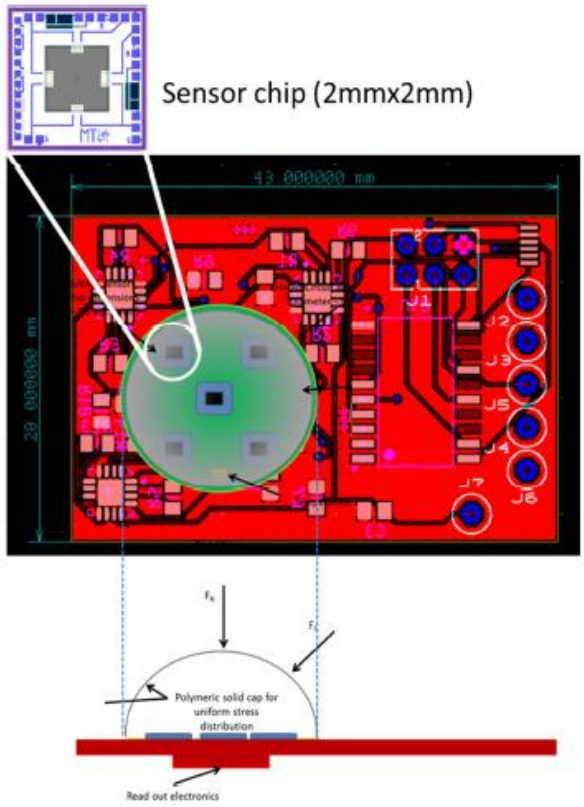


Figure 1 Schematic of the sensor unit: layout of the sensor chip (top) and cross section of the PCB (bottom)

For the sensor chip, it is designed as a single device being assembled on a PCB with one central and four peripheral sensors. The peripheral are required for the detection of shear forces acting on the polymeric dome.

The piezoresistive sensors (the central one and the four peripheral sensors) of the chip have been tested upon incremental weight of 700g and the experimental data have been extracted for providing the calibration curves. The data, as already reported elsewhere [9], shows a good linearity in the range of 0 - 2 Kg (corresponding to 0-396 kPa for a contact area of 0.2 $cm^2$), with a sensitivity to the normal force of about 3mV/g for the central sensor of the chip and of 0.5 mV/g for the peripheral sensors.

### *B. Design of integrated sensor socket*

Figure 2 shows the top view of the integrated sensor socket system (MasterSocket) which consists of 36 adjustable sensor pads that are used to support the stump's volume part in its medium and lower areas.

The upper part of the stump is handled by the MasterSocket's specifically adjustable brim parts and their role is to support up to 60-70% of the body weight of the amputee. The brim parts are 3D printed, each has special holes for cable routing and screw inserts integration. In our current design, each brim part has at least three tri-axial normal and shear force sensors to provide the load on the socket brim.

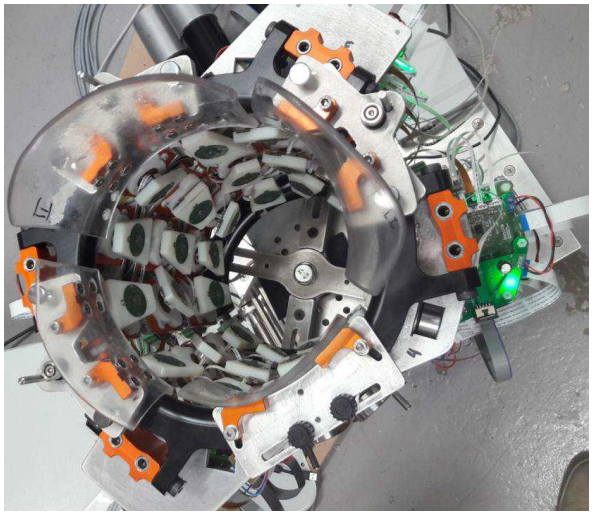

Figure 2 Top view of the master socket system

Although the middle and lower part of a stump only carries less than 40% of the body weight, anatomically this part is under more shear load than the upper part. Therefore, the adjustability of this part is more important than the upper part.

Figure 3 shows a sensor assembly with sensor dome, PCB and pad. In order to adjust the position of the sensor pad to suit different dimensions of amputee's residual limbs, the position of each sensor assembly is controlled by a linear actuator. The linear actuator assembly not only provides the position adjustment, but also recorded the movement of the sensor assembly which provides displacement reading in relation to the forces measured by the sensor.

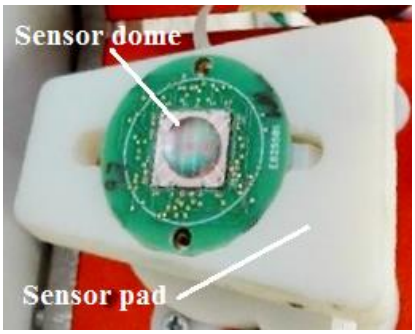


Figure 3 Sensor assembly

Apart from the sensor dome, the surface of PCB and sensor pad will be covered by a flat panel which provides smooth contact with soft tissue.

When a residual limb is placed in the master socket (as shown in Figure 2), not only the sensor dome, but also the flat panel will be in contact with residual limb. Since only the dome part of sensor assembly can provide pressure readings, we need to find a way of reconstructing the average surface pressure over the area of the flat panel before the surface pressure on the residual limb is reconstructed.

### *C. Surface Pressure Reconstruction*

As described above, although the SocketMaster system employed 36 adjustable pads, there are two issues needs to be addressed so that a detailed pressure distribution can be obtained from the system. The first issue is how to provide overall pressure distribution on the residual limb with only 36 individual sensors. The second issue is, for each sensor, only the sensor area (dome part) provides pressure readings. When the sensor flat panel is in contact with residual limb there will be an unmeasurable pressure on the flat panel area.

In order to establish a relationship between the pressure measured by each individual sensor and the average pressure on the flat panel area, we used finite element simulation to determine the average surface stress in this areas, as it is more cost effective than using an experiment method.

The simulations can provide stresses on both dome (sensing) area and flat panel (non-sensing) area for the sensor assembly while it is pushed toward to the residual limb. As a case study, the effect of a bone in the soft tissue was not considered in the current study.

Based on the simulation result we establish a relationship between the pressure measured by each individual sensors and average pressure on the flat panel. Eventually, the overall pressure distribution on the residual limb could be reconstructed from the average pressure of 36 flat panel of the SocketMaster system.

## III. NUMERICAL SIMULATION

As the purpose of this study is to describe the basic approach and to address any potential issues, a simplified sensor and soft tissue finite element model is used as a case study.

### *A. Numerical simulation model*

Figure 4 shows the finite element model used in our simulation. It has a cylindrical base material and a sensor assembly. The diameter of the base material is 120mm with thickness 50mm. The profile of the sensor is an ellipse generated by an 8 mm diameter sphere protruding 3 mm from the pad surface. The dimensions of the sensor pad are 40 ×30 ×5 mm. The lowest point of the sensor body is placed 0.01 mm above the top surface of the base material.

The sensor is simulated as a rigid body and the base material is simulated as a hyperelastic Ogden model based on the experiment shown in Table 1[10].

Table 1 Experimental data (stress in MPa)

| | | | | | | |
|---|---|---|---|---|---|---|
| σ | 0 | 0.009 | 0.015 | 0.02 | 0.024 | 0.027 |
| ε | 0 | 0.2 | 0.4 | 0.6 | 0.8 | 1.0 |

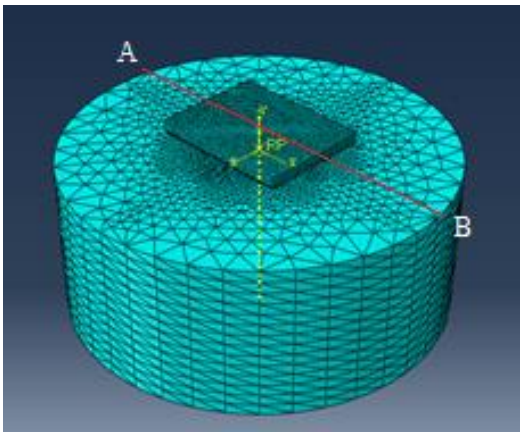


Figure 4 Finite element model

The base material is constrained in all 6 DOF on its bottom surface and the sensor assembly is moved toward to the base material. The top surface of the base material is assigned as the slave of the surface to surface interaction.

### *B. Simulation and data processing procedures*

Abaqus/CAE (Dassault Systèmes® 2017) was used to simulate the interaction process between the sensor assembly and base material. The simulations were carried out in two steps.

The first step is to move the sensor assembly down by 3.01 mm, where the bottom surface of the flat panel is in line with the initial position of the top surface of the base material and the elliptic part of sensor is pushed into the base material by 3mm in depth. Through the simulation, the stress on the sensor can be obtained.

The second step is to move the sensor assembly down another 2 mm. At the end of this step, the bottom surface of the flat panel is pushed into the base material by 2 mm in depth. Through this simulation, the stress on both sensor and flat panel around the sensor can be obtained.

Convergence test was carried out to determine the optimum size of elements and the model was meshed with tetrahedron element with total around 50 k nodes.

A path AB is defined across the base material as shown in Figure 4. Along this path, the stresses and displacements in the direction of the sensor movement are recorded.

From the recorded stresses on both the sensor and flat panel, an average stress is calculated to represent the equivalent stress at different positions on the sensor/flat panel during the movement from 0 to 5.01 mm.

It should be noted that the actual geometry of the residual limb is much more complex than the base material we used for this study. However, the purpose of this study is to explore the relationship between the sensor / flat panel displacement and the stress produced in the soft tissue, the simplified case study should be sufficient to validate the approach we used.

## IV. Simulation Results

### A. *Stresses on the Sensor*

Figure 5 shows a cross section view of stress distribution in the direction of sensor movement, when the sensor is pushed down 3.01 mm into the base material.

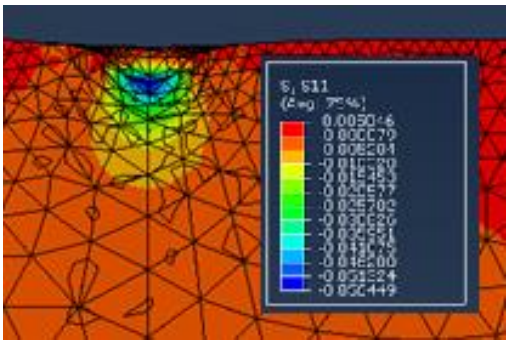

Figure 5 Stress distribution sensor at 3.01mm

Table 2 shows the average stress within the sensor area against the displacement when the sensor/flat panel is moved down by 3.01mm.

Table 2 Average stress on sensor

| Displacement | 0 | 1.01 | 2.01 | 3.01 |
|---|---|---|---|---|
| Stress (-kPa) | 0 | 9.4 | 18.9 | 28.2 |

Table 3 shows the average stress within the sensor area against the displacement when the sensor/flat panel is moved from 3.01 mm to 5.01 mm.

Table 3 Average and maximum stress on sensor (-kPa)

| Displacement | 3.01 | 3.51 | 4.01 | 4.51 | 5.01 |
|---|---|---|---|---|---|
| Stress (Max) | 53.8 | 58.7 | 62 | 64 | 65.5 |
| Stress (Avg) | 28.2 | 32.4 | 35 | 36.7 | 37.8 |
| Ratio | 52.4% | 55.2% | 56.5% | 57.3% | 57.7% |

Figure 6 shows the average stress in the sensor area against the displacement of sensor from 0 to 5.01 mm.

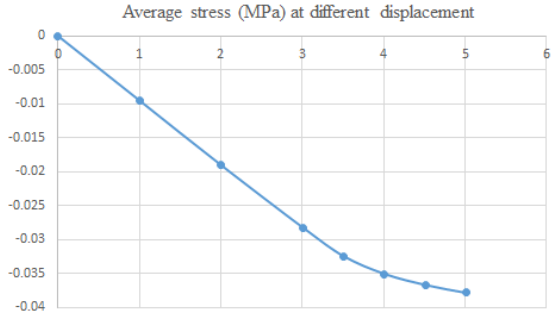


Figure 6 Average stress in the sensor area

### B. *Stress on the flat panel*

Table 4 shows the average stress against the displacement in the flat panel area when sensor assembly is moved from 3.01 mm to 5.01 mm.

Table 4 Average stress on flat panel

| Displacement | 3.01 | 3.51 | 4.01 | 4.51 | 5.01 |
|---|---|---|---|---|---|
| Stress (-kPa) | 0 | -0.87 | -1.82 | -3.33 | -4.82 |

Figure 7 shows the stress distribution along the path AB at sensor positions between 3.01mm to 5.01mm.

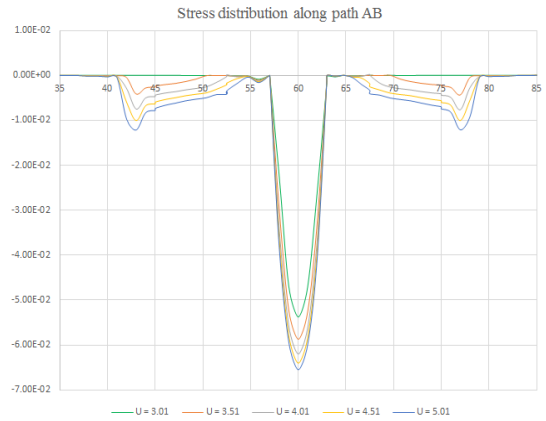


Figure 7 Stress distribution along path AB

Table 5 shows the percentage ratio of the average stress in flat panel area against average stress in the sensor area.

Table 5 Average Pad/Sensor stress ratio

| Displacement | 3.01 | 3.51 | 4.01 | 4.51 | 5.01 |
|---|---|---|---|---|---|
| Flat panel: Sensor Ratio | 0.00% | 3.28% | 6.62% | 9.64% | 12.10% |

Figure 8 shows average stress percentage ratio in the flat panel area against the average stress in the sensor area between sensor displacements of 3.01 mm to 5.01 mm.

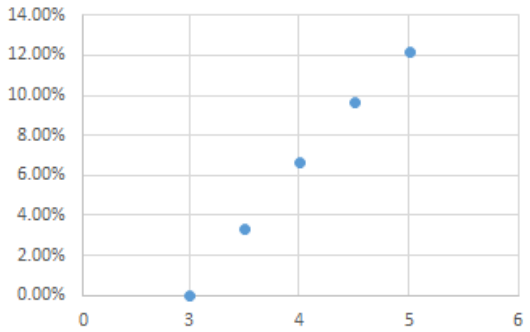


Figure 8 Average stress percentages

## VI. Discussion and Conclusion

### A. Average stress in the sensor area

The simulation results shown in Table 2 indicates that there is a linear relationship between the indentation displacement and average stress in the sensor area before the flat panel is in contact with the base material.

Table 3 shows that both the maximum stress and average stress in the sensor area increase with indentation displacement. The ratio between the maximum and average stress also increases with displacement.

The simulation results shown in Table 3 also indicate that, from 3.01 to 5.01 mm, the relationship between the indentation displacement and average stress in the sensor area becomes non-linear.

The curve in Figure 6 displays a clear trend that, with an increase of the indentation displacement from 3.01 to 5.01 mm, the stress in the sensor area quickly drops. Because of this trend, a further indentation displacement is likely to make the pressure changes in the sensor area undetectable.

### B. Average stress in the pad area

The simulation results shown in Table 4 indicates that there is a close to linear relationship between indentation displacement and average stress in the flat panel area after it is in contact with the base material.

The simulation results shown in Figure 7 indicate that the stress distribution in the flat panel area appears to be non-uniform. A large change can be found around the edge of the flat panel and the area close to the sensor. This is the reason that in this study average values are used to establish the relationship between the stress measured by the sensor and the stress in the flat panel area.

Table 5 shows the ratios in percentage between average pressures in the sensor and flat panel areas after the flat panel is in contact with base material. Figure 8 indicates that the ratio increases with indentation displacement with slight nonlinearity between 3.01 and 5.01mm.

### C. Method of surface pressure reconstruction

The main propose of this study is to reconstruct the pressure distribution over the residual limb from the pressure measured by 36 individual sensors. As described in the introduction of this paper, after the flat panel is in contact with soft tissue, the reading from the sensor cannot represent the true pressure on the residual limb. Establishing the relationship between the stress on the sensor and the average stress in the flat panel can help us to solve this issue.

From the simulation result shown in Table 5, a relationship between two can be established through a regression process. In result, a relationship can be represented using a second order polynomial equation.

$$R = -0.0056d^2 + 0.106\,d - 0.269 \qquad (1)$$

where $R$ is the stress ratio between the sensor and flat panel area and, $d$ is the indentation displacement.

Clearly, this relationship is only valid after the sensor pad is in contact with soft tissue (base material in this case study). As Figure 6 indicates, with the increase of the indentation displacement, the pressure change on the sensor will approach to zero. Therefore, it is reasonable assumption that the above derived relationship may not be applicable when the indentation displacement reaches certain limit.

### D. Conclusion and limitation

Using the numerical based reverse engineering method, this study concludes that, before the sensor pad is in contact with the base material (soft tissue), there is a linear relationship between indentation displacement and stress on the soft tissue within the area of the sensor dome.

However the relationship becomes nonlinear after the flat panel is in contact with soft tissue. The study shows that, once the elastic modulus is given, such a relationship can be represented by a second order polynomial equation and used to determine the average pressure within the area of the flat panel.

As a case study, the simulation confirms the feasibility of reconstructing pressure distribution over a residual limb for the

SocketMaster system using pressure readings from 36 individual sensors as shown in Figure 2.

It should be noted that there are some limitations with the current study. The first one is that variation of the base material is not considered in this case study. When the elastic modulus of the base material, i.e. soft tissue in a case of real clinical application, is changed, coefficients of the regression equation, which represents the ratio between the average pressure on the sensor and in the flat panel area, would be different.

The second limitation is the location of the bone in the current study. When the bone is close to the surface of the soft tissue, it would change the simulation result significantly.

To overcome the above limitations, further simulations could be carried out with different elastic moduli and location of the bone.

## ACKNOWLEDGMENT

The authors would like to acknowledge the funding support from the EU Horizon 2020 (645239) project. The authors also would like to acknowledge the contributions to the sensor development from the other partners of the SocketMaster project consortium.

## REFERENCES

[1] P. Botta, R. Baumgartner "Socket design and manufacturing technique for through-knee stumps" Prosthetics and Orthotics International, 7(2), pp. 100-3, Aug 1983.

[2] T. Chin, K. Machida, S. Sawamura, R. Shiba, H. Oyabu, Y. Nagakura, I. Takase, A. Nakagawa, Comparison of different microprocessor controlled knee joints on the energy consumption during walking in trans-femoral amputees: Intelligent Knee Prosthesis (IP) versus C-Leg" Prosthetics and Orthotics International, vol. 20, no. 1, pp. 73-80, 2006.

[3] D.L. Bader, C. Bouten, D. Colin, C.W.J. Oomens "Pressure Ulcer Research (1st ed.)," Springer-Verlag, Berlin, pp. 129-147

[4] P. Laszczak, M. McGrath, J. Tang, J. Gao, L. Jiang, D. L. Bader, D. Moser, S. Zahedi "A pressure and shear sensor system for stress measurement at lower limb residuum/socket interface" Medical Engineering and Physics 38 (2016) 695–700

[5] W. Xu, A. S. Haidar, L. Lorenzelli, V. Papadimitriou, C. Alcobia, R. Pierobon, R. Lopatka, J. Gao, "Development of a SocketMaster system for optimising the design of prosthetic socket for above knee amputees" The ISPO World Congress, Cape Town, SA, 5-8 May 2017

[6] W. Xu, A. S. Haidar, L. Lorenzelli, V. Papadimitriou, C. Alcobia, R. Pierobon, R. Lopatka, J. X. Gao "Use of tissue indentation method for the evaluation of residual limbs" ISB2017, Australia, Brisbane, 23 - 27 July 2017

[7] G. Sordo, L. Lorenzelli, "Design of a novel tri-axial force sensor for optimized design of prosthetic socket for lower limb amputees," Proc. of DTIP 2016 (Symposium on Design, Test, Integration and Packaging of MEMS and MOEMS), 2016, pp. 51- 54.

[8] R. Maurizio, L. Leandro, A. Rizzi, B Davide, "Portable embedded systems for prosthetic interface stress mapping of lower limbs amputees" IEEE Sensors, Orlando, FL, USA, 30 Oct – 2 Nov 2016.

[9] Leandro Lorenzelli, et al." Socketmaster: Integrated Sensors System for the Optimised Design of Prosthetic Socket for above Knee Amputees", Published in: CAS (NGCAS), 2017 New Generation of, 6-9 Sept. 2017, pp. 233-236.

[10] W. Xu, A. S. Haidar, J. Gao, "Study of Biomechanical Model for Smart Sensor Based Prosthetic Socket Design System", World Academy of Science, Engineering and Technology International Journal of Bioengineering and Life Sciences, Vol:12, No:1, 2018